Phonon Softening in Individual Metallic Carbon Nanotubes due to the Kohn Anomaly

H. Farhat,[1] H. Son,[2] Ge. G Samsonidze,[3] S. Reich,[4] M. S. Dresselhaus,[2] and J. Kong[2]

[1]*Department of Materials Science and Engineering, MIT, Cambridge, Massachusetts 02139, USA*

[2]*Department of Electrical Engineering and Computer Science, MIT, Cambridge, Massachusetts 02139, USA*

[3]*Department of Physics, University of California at Berkeley, Berkeley, California 94720-7300, USA*

[4]*Fachbereich Physik, Freie Universitt Berlin, D-14195 Berlin, Germany*

(Received 4 May 2007; revised manuscript received 30 July 2007; published 5 October 2007)

We have studied the line shape and frequency of the *G* band Raman modes in individual metallic single walled carbon nanotubes (M-SWNTs) as a function of Fermi level (ϵ_F) position, by tuning a polymer electrolyte gate. Our study focuses on the data from M-SWNTs where explicit assignment of the G^- and G^+ peaks can be made. The frequency and line shape of the G^- peak in the Raman spectrum of M-SWNTs is very sensitive to the position of the Fermi level. Within $\pm\hbar\omega/2$ (where $\hbar\omega$ is the phonon energy) around the band crossing point, the G^- mode is softened and broadened. In contrast, as the Fermi level is tuned away from the band crossing point, a semiconductinglike *G* band line shape is recovered both in terms of frequency and linewidth. Our results confirm the predicted softening of the *A*-symmetry LO phonon mode frequency due to a Kohn anomaly in M-SWNTs.

Recent experimental and theoretical studies on single wall nanotubes (SWNTs) have reported significant electron-phonon (*e-p*) interactions in electrical transport [1,2], electron tunneling [3], and optical transitions [4–6]. An investigation of the *e-p* coupling mechanisms in metallic nanotubes is therefore fundamental to understanding 1D conduction in these materials. Electron-phonon coupling has been predicted to give rise to a striking difference between the *G* band Raman feature of metallic (M) and semiconducting (S) SWNTs [7–11]. The lower energy (G^-) peak of M-SWNTs (M-G^-) typically is much broader and occurs at a lower frequency compared to the G^- peak in S-SWNTs (S-G^-), and in some cases exhibits an asymmetric line shape. While the S-G^- has been assigned to the transverse optical (TO) phonon mode, which is downshifted with respect to the S-G^+ due to the SWNT curvature, several recent works [7–11] have assigned M-G^- to the longitudinal optical (LO) mode with *A* symmetry, softened by a Kohn anomaly (KA) at the Γ point in the phonon dispersion.

The KA occurs in the LO phonon branch because the LO phonon distorts the lattice such that a dynamic bandgap is induced in the electronic band structure [8]. This lowers the energy of the valence electrons near the Fermi point and thus lowers the energy required to distort the lattice, leading to phonon softening. Clearly, this coupling mechanism is sensitive to the position of the Fermi level. As the Fermi level (ϵ_F) is shifted away from the Fermi point, the electronic energy saved by distorting the lattice becomes negligible. Moving ϵ_F by means of doping or a gate voltage therefore provides a way of tuning the strength of the electron-phonon coupling.

A large body of work has been carried out on this topic, whereby ϵ_F of SWNTs was tuned by alkali metal doping [12–14], polymer doping [15], and by electrochemical gating [16–21]. A general trend of an increase in the frequency and a decrease in the linewidth of the M-G^- peak was observed for both *n*-type and *p*-type doping. However, since most of these studies were carried out on large ensembles of nanotube bundles, it was not possible to track individual peaks as a function of doping. Even in studies carried out at the individual M-SWNT level [22], the *G* band often contains several overlapping peaks, making it difficult to assign and track each peak as ϵ_F is tuned.

In this Letter we used a polymer electrolyte gate to tune ϵ_F in order to study the KA in individual M-SWNTs. We show that, among the many M-SWNTs investigated, some M-SWNTs have only two peaks (G^- and G^+) in their *G* band Raman spectrum when ϵ_F is tuned from the band crossing point to high positive or negative doping levels. For these nanotubes, we are able to unambiguously track the position of the G^- peak and observe the evolution of its line shape and frequency as a function of ϵ_F. The results of our analysis are in good *quantitative* agreement with recent theoretical predictions of phonon softening in M-SWNTs by a KA mechanism [11]. Our observations provide convincing evidence of the existence of a KA in the *A* symmetry LO phonon branch of individual M-SWNTs.

SWNTs were grown by CVD (chemical vapor deposition) on a SiO_2/Si substrate using dispersed catalytic ferritin nanoparticles. Subsequently, a 30 nm Au ground electrode with a Cr adhesion layer was evaporated on half of the substrate to keep the nanotubes at a constant potential with respect to the gate [Fig. 1(a)]. The SWNT density was kept high enough to create a network of tubes that are connected to the ground electrode, but low enough to be able to observe spectra from individual tubes with a laser spot size of $\sim 1 ~\mu$m. Figure 1(b) is a representative atomic force microscope (AFM) image of the samples used in this work. To get a high gating efficiency, we used a molten
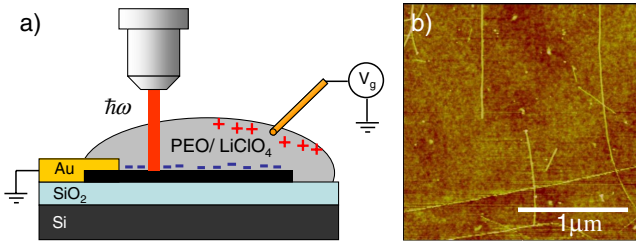
FIG. 1 (color online). (a) Schematic diagram of the experimental setup. The excitation laser shines through the PEO/LiClO$_4$ polymer electrolyte. (b) An AFM image indicating that the nanotubes are spaced out and are typically isolated from one another.

polymer electrolyte [23,24] that is stable under applied voltages greater than 1 V. A gold wire was used to apply a voltage to the polymer gate. Raman spectra were taken at a laser energy (E_{laser}) of 1.91 eV (647 nm) with a spectrometer resolution of ~5 cm^{-1}. A ~1 μm laser spot was scanned along the edge of the ground electrode in search of M-SWNTs [based on the radial breathing mode (RBM) frequency or the G band line shape]. Once the desired SWNT was located, a series of spectra were taken while sweeping the gate voltage. Raman modes of the electrolyte (1450 and 1485 cm^{-1}) are also present in the region of interest and can overlap with the tail of the broadened G band. However, these peaks are independent of the applied gate voltage V_G and are easily distinguished from the G band signal. All of the nanotubes that we have studied exhibit a weak or absent D band, whose intensity and frequency are independent of V_G.

Figure 2(a) is a representative map of the G band intensity of a M-SWNT as a function of the gate potential V_G. A clear evolution of the M-G^- and M-G^+ peaks can be seen. The M-G^- peak shifts almost symmetrically about $V_{G,o} = 1.2$ V [Fig. 2(a)]. The G band spectra, for the same nanotube at various gate voltages, are shown in Fig. 2(b). Here we see that at $V_{G,o}$, M-G^- has the lowest frequency (1550 cm^{-1}) and amplitude as well as the greatest full width at half maximum (FWHM) (68 cm^{-1}). We believe that $V_{G,o}$ corresponds to zero doping (i.e., the band crossing point), since nanotubes are usually p type from ambient oxygen doping and can be further doped by the electrolyte solution due to perchlorate adsorption on the nanotubes [25]. When the gate voltage is moved below or above $V_{G,o}$, the M-G^- peak frequency and intensity increase, its linewidth decreases, and the peak line shape becomes similar to the G band of S-SWNTs [Fig. 2(b)]. On the other hand, the M-G^+ peak in this sample (located at 1589 cm^{-1} for $V_G \sim V_{G,o}$), only upshifts by 18 cm^{-1} with no appreciable change in FWHM for the same range of electrochemical gating V_G. The intensity of the M-G^+ peak is significantly reduced when V_G is moved away from $V_{G,o}$, showing a sharp contrast to the response of the M-G^- peak to changes in the ϵ_F position.
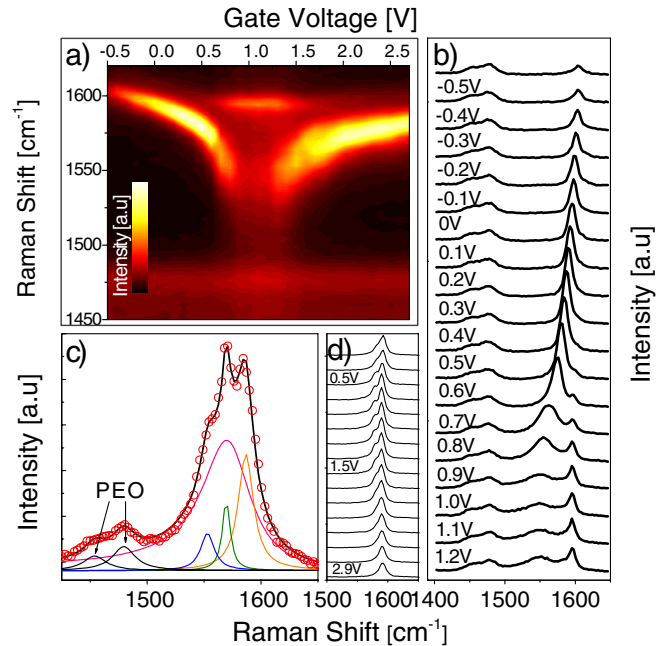
FIG. 2 (color online). (a) G band intensity map vs applied gate voltage V_G for an individual M-SWNT. (b) G band spectrum, for the same nanotube as in (a), taken at the indicated V_G values. The spectrum at the bottom of the panel corresponds to $V_{G,o}$. (c) G band of a M-SWNT whose peaks are difficult to track because the spectrum is composed of many overlapping peaks. Arrows indicate peaks associated with the electrolyte (d) G band of a S-SWNT taken at the different V_G, with a step in V_G of 0.2 V between traces.

For SWNTs, the G band has six components corresponding to TO and LO phonon modes, each with either A, E_1, or E_2 symmetry [26]. The A symmetry modes typically make the largest contribution to the intensity [27]. For the M-SWNT shown in Figs. 2(a) and 2(b), the G band spectrum exhibits only two peaks throughout the range of electrochemical gating. In addition, the peak intensities and positions evolve gradually and smoothly when the ϵ_F position changes, without any sudden shifts or abrupt jumps. Furthermore, when the M-G^- peak shifts, it carries all of its intensity with it, without leaving behind another peak. Based on all the above, we believe that the M-G^- and M-G^+ peaks can definitively be assigned to the A symmetry LO and TO modes, respectively. In some nanotubes it is difficult to easily assign modes to the peaks because there are multiple peaks in the G band spectrum. Figure 2(c) is an example of the spectrum for one such tube taken at $V_G \sim V_{G,o}$ (see also [22]). When V_G is moved away from $V_{G,o}$, some peaks overlap and others disappear entirely, making it difficult to correctly assign the peaks and to track their evolution. The explicit assignment of the peaks shown in Fig. 2(b) allows us to focus on the evolution of the M-G^- peak under gating, which has been proposed to be softened by a KA mechanism. We have performed a quantitative comparison with theoretical mod-

els in terms of the frequency change and linewidth. A number of works have calculated the renormalized LO phonon dispersion due to the KA, using density functional theory [8,10,11] and tight-binding methods [9,28], with [9,11] specifically addressing the dependence of the phonon softening on the ϵ_F position. Recent works addressing the time dependence of the coupling mechanism have demonstrated that there are significant corrections to the phonon renormalization with respect to calculations that treat the problem in the static approximation [11,29]. Here we compare our data to an analytical result taken from [11] where a time-dependent dynamical matrix is used to determine the renormalized phonon frequency and lifetime.

Figure 3(a) shows the measured frequency vs ϵ_F for two different M-SWNTs (for which only two peaks were observed in the G band) laid over the calculated phonon frequencies based on [11]. The only fitting parameter is the gate coupling efficiency, taken as 0.4 and 0.37 for M-SWNT #1 and #2, respectively. These values are slightly lower than the gating efficiency of 0.6 previously reported for this type of gating setup [30]. In our calculation, we have used a tube diameter of 1.2 nm, since we observe a RBM frequency mostly in the range of 190–205 cm^{-1} with an excitation energy of 1.91 eV. The two minima, located at $\pm\hbar\omega/2$ on the solid curve in Fig. 3(a), correspond to ϵ_F being equal to half the phonon energy, at which point the e-p coupling is the strongest because the energy of the electronic intraband excitations is exactly the phonon energy. These singularities appear in the calculated phonon frequency for a perfect crystal at a temperature of $T = 0$ K. However, with higher T, and energy level broadening due to disorder, we do not expect to see these singularities in our experiment [11].

Various decay pathways contribute to the phonon linewidth. The total linewidth is given by $\Gamma_{TOT} = \Gamma_{EPC} + \Gamma_0$

where Γ_{EPC} is the gate-dependent contribution from e-p coupling and Γ_0 includes contributions from phonon-phonon interactions, inhomogeneous broadening, and impurity scattering. Γ_{EPC} arises from the decay of the LO phonon into low energy electron or hole excitations near the Fermi surface, hence reducing the phonon lifetime [31]. Once $|\epsilon_F| > \hbar\omega/2$, there are no longer allowable electron or hole intraband excitations, and therefore there is a sudden decrease in the linewidth. Figure 3(b) shows Γ_{EPC} as a function of V_G for the two M-SWNTs in Fig. 3(a) overlaid with the theoretical Γ_{EPC} from Ref. [11]. Γ_0 is taken as 12 and 10 cm^{-1} for M-SWNT #1 and #2, respectively, which are obtained from the linewidth at high negative gate voltages, where the linewidth no longer changes with gate voltage.

The quantitative agreement between our data and the theoretical calculations provides compelling evidence that the M-G^- peak is softened due to a KA in the phonon dispersion of M-SWNTs. In addition, the KA mechanism predicts that out of the 6 modes in the G band, only the A symmetry LO mode will have this dramatic frequency shift due to e-p coupling. This is also consistent with our observations. In Fig. 3(a) the frequencies of the M-G^+ from the two M-SWNT samples are also plotted versus the ϵ_F position. Over a wide energy range around the band crossing point, there is hardly any change in the frequency of the M-G^+ peak. At higher negative or positive V_G, M-G^+ begins to harden (upshift in frequency), but the range of frequency shift for different M-SWNTs is only 5–20 cm^{-1}, which is much less than what is predicted by a KA mechanism.

We suspect that the hardening of M-G^+ under high positive or negative gating is a result of the electromechanical effect due to charge injection [32]. We have observed a similar behavior in the G band of some S-SWNTs. However, S-SWNTs are not predicted to be affected by a KA, and indeed we do not observe large shifts in the G band of S-SWNTs. In Fig. 2(d), the evolution of a S-SWNT G band is shown. Typically, at high doping levels, there is a decrease in G band intensity (S-G^- or S-G^+, or both), accompanied by a small upshift in frequency of ~3–5 cm^{-1}. In certain S-SWNTs, however, the frequency hardening can be up to 20 cm^{-1}. These characteristics are similar to what is observed for the M-G^+ peaks, but are distinctly different from the behavior of the M-G^- peak.

Although both M-SWNTs in Fig. 3 exhibit a similar frequency and linewidth behavior, when V_G is near the Fermi point, M-SWNT #2 exhibits a Fano line shape while M-SWNT #1 is well fitted to a Lorentzian for all V_G. This is consistent with [31], where different values of the asymmetry parameter ($1/q$) in the Fano line shape are reported for different (n, m) metallic nanotubes. The value of $-1/q$ for M-SWNT #1, plotted as a function of ϵ_F in Fig. 3(c), decreases from 0.15 to 0.04 as the Fermi level is shifted

FIG. 3 (color online). (a) Frequency of M-G^+ (open points) and M-G^- (filled points), (b) linewidth Γ_{EPC} of M-G^-, and (c) $-1/q$ of M-G^- as a function of the Fermi level for two M-SWNT [tube 1 dots, tube 2 triangles]. Γ_0 is taken as 12 and 10 cm^{-1} for tubes 1 and 2, respectively. The solid lines in (a) and (b) are the calculated frequencies ($T = 0$ K) and linewidths ($T = 300$ K) of the LO A symmetry phonon from Ref. [11].

away from the Fermi point. The curve shape in Fig. 3(c) follows the variation of frequency [Fig. 3(a)] and linewidth [Fig. 3(b)] very well, indicating that the degree of asymmetry correlates with the strength of the e-p coupling. However, although it appears that the asymmetry is mediated by the same e-p coupling mechanism that induces the KA, because the G^- of M-SWNT #1 does not show any asymmetry throughout the gating range, the e-p coupling alone is evidently not sufficient to create a Fano resonance. The Fano line shape is a result of interference between Raman scattering of the LO phonon and electronic Raman scattering from the continuum of electronic excitations [33]. The parameter q is defined by $q = \pi V_{e\text{-}p} R_p / R_e$ [33] where $V_{e\text{-}p}$ is the electron-phonon coupling matrix element and R_p and R_e are the Raman tensors for phonon and electron scattering, respectively. We expect the ratio R_p / R_e to depend on the (n, m) values of the nanotube. Furthermore, since the phonon and electron Raman scattering processes have different resonance profiles, the ratio R_p / R_e is also likely to depend on E_{laser}. We are currently investigating the dependence of the M-G^- line shape on E_{laser}.

In summary, we have studied the e-p coupling due to a KA in individual M-SWNTs by observing the evolution of the G band Raman spectrum while applying an electrochemical gate voltage. In M-SWNTs where only two peaks are observed in the G band spectra throughout the gating range, the peaks were unambiguously assigned and their behavior upon gating, in terms of frequency, linewidth, and line shape, was investigated. Our experimental data provide convincing evidence of the KA phenomenon in M-SWNTs and are in good quantitative agreement with theoretical calculations [10]. A similar experiment was carried out previously [22], but no clear evidence of a KA was observed. This is most likely due to the presence of multiple peaks in the G band [Fig. 2(c)]. Our results indicate that other G band peaks also show a dependence on ϵ_F. However, the changes in intensity and frequency for these modes are different from what is observed for the A symmetry LO mode and are not well understood at present. In the case when these peaks overlap with the A-symmetry LO phonon mode [22], it is difficult to follow this mode quantitatively and to observe its softening by the KA. Our current understanding of the response of the A symmetry LO phonon mode under gating provides guidance for assigning peaks in the multipeak G band spectra, creating opportunities for further study of the ϵ_F dependence of other G band features in M-SWNTs.

[1] J. Y. Park *et al.*, Nano Lett. **4**, 517 (2004).
[2] E. Pop *et al.*, Phys. Rev. Lett. **95**, 155505 (2005).
[3] S. Sapmaz *et al.*, Phys. Rev. Lett. **96**, 026801 (2006).
[4] S. G. Chou *et al.*, Phys. Rev. B **72**, 195415 (2005).
[5] Y. Miyauchi and S. Maruyama, Phys. Rev. B **74**, 035415 (2006).
[6] F. Plentz *et al.*, Phys. Rev. Lett. **95**, 247401 (2005).
[7] E. Di Donato, M. Tommasini, C. Castiglioni, and G. Zerbi, Phys. Rev. B **74**, 184306 (2006).
[8] O. Dubay, G. Kresse, and H. Kuzmany, Phys. Rev. Lett. **88**, 235506 (2002).
[9] G. G. Samsonidze *et al.*, Phys. Rev. B **75**, 155420 (2007).
[10] S. Piscanec *et al.*, Phys. Rev. B **75**, 035427 (2007).
[11] N. Caudal, A. M. Saitta, M. Lazzeri, and F. Mauri, Phys. Rev. B **75**, 115423 (2007).
[12] N. Bendiab *et al.*, Phys. Rev. B **64**, 245424 (2001).
[13] L. Grigorian *et al.*, Phys. Rev. Lett. **80**, 5560 (1998).
[14] A. M. Rao *et al.*, Nature (London) **388**, 257 (1997).
[15] M. Shim, T. Ozel, A. Gaur, and C. Wang, J. Am. Chem. Soc. **128**, 7522 (2006).
[16] P. Corio *et al.*, Chem. Phys. Lett. **370**, 675 (2003).
[17] S. B. Cronin *et al.*, Appl. Phys. Lett. **84**, 2052 (2004).
[18] L. Kavan, L. Dunsch, and H. Kataura, Carbon **42**, 1011 (2004).
[19] L. Kavan *et al.*, J. Phys. Chem. B **105**, 10 764 (2001).
[20] P. M. Rafailov, J. Maultzsch, C. Thomsen, and H. Kataura, Phys. Rev. B **72**, 045411 (2005).
[21] M. Stoll, P. M. Rafailov, W. Frenzel, and C. Thomsen, Chem. Phys. Lett. **375**, 625 (2003).
[22] K. T. Nguyen, A. Gaur, and M. Shim, Phys. Rev. Lett. **98**, 145504 (2007).
[23] G. P. Siddons *et al.*, Nano Lett. **4**, 927 (2004).
[24] C. G. Lu, Q. Fu, S. M. Huang, and J. Liu, Nano Lett. **4**, 623 (2004).
[25] M. Kruger *et al.*, Appl. Phys. Lett. **78**, 1291 (2001).
[26] C. Thomsen, S. Reich, P. M. Rafailov, and H. Jantoljak, Phys. Status Solidi **214**, r15 (1999).
[27] A. Jorio *et al.*, Phys. Rev. Lett. **90**, 107403 (2003).
[28] V. N. Popov and P. Lambin, Phys. Rev. B **73**, 085407 (2006).
[29] K. Ishikawa and T. Ando, J. Phys. Soc. Jpn. **75**, 084713 (2006).
[30] T. Ozel, A. Gaur, J. A. Rogers, and M. Shim, Nano Lett. **5**, 905 (2005).
[31] Y. Wu *et al.*, Phys. Rev. Lett. **99**, 027402 (2007).
[32] A. Z. Hartman, M. Jouzi, R. L. Barnett, and J. M. Xu, Phys. Rev. Lett. **92**, 236804 (2004).
[33] M. Cardona, F. Cerdiera, and T. Fjeldly, Phys. Rev. B **10**, 3433 (1974).